Volume 6, Issue 6, 2016, 1702 - 1709 ISSN 2069-5837

Biointerface Research in Applied Chemistry

www.BiointerfaceResearch.com

Original Research Article Open Access Journal

Received: 20.10.2016 / Revised: 07.11.2016 / Accepted: 08.11.2016 / Published on-line: 09.11.2016

Green synthesis of red-fluorescent gold nanoclusters: characterization and application for breast cancer detection

Agnė Mikalauskaitė [1], Vitalijus Karabanovas [2], Renata Karpicz [3], Ričardas Rotomskis [2], Arūnas Jagminas[1,*]

[1] Department of Electrochemical Material Science, Center for Physical Sciences and Technology, Vilnius, Lithuania
[2] Biomedical Physics Laboratory, National Cancer Institute, Vilnius, Lithuania
[3] Department of Molecular Compound Physics, Center for Physical Sciences and Technology, Vilnius, Lithuania

*corresponding author e-mail address: ***arunas.jagminas@ftmc.lt***

ABSTRACT

The use of biocompatible precursors for the synthesis and stabilization of fluorescent gold nanoclusters (NCs) with strong red photoluminescence creates an important link between natural sciences and nanotechnology. Herein, we report for the first time the cost-effective synthesis of Au nanoclusters by templating and reduction of chloroauric acid with the cheap amino acid food supplements. This synthesis under the optimized conditions leads to formation of biocompatible Au NCs having good stability and intense red photoluminescence, peaked at 680 to 705 nm, with a quantum yield (QY) of ≈7% and average lifetime of up to several μs. The composition and luminescent properties of the obtained NCs were compared with ones formed via well-known bovine serum albumin reduction approach. Our findings implied that synthesized Au NCs tend to accumulate in more tumorigenic breast cancer cells (line MDA-MB-213) and after dialysis can be prospective for bio imagining.

Keywords: *gold nanoclusters, proteins, materials chemistry, red-photoluminescence, bio imaging.*

1. INTRODUCTION

In the past decade, ultra-small gold nanoparticles (USNps) [1], 1 to 3 nm in size, and nanoclusters (NCs) [2], ≤ 1.5 nm in size, have received a great deal of attention because they can exhibit strong photoluminescence and, in contrast to semiconducting fluorescent quantum dots, comprised mainly of cadmium selenides and tellurides [3-5], are nontoxic in vivo and biocompatible. It should be noted, however, that to achieve strong photoluminescence of gold NCs and USNps nearly monodisperse size distribution is required because the addition of even one atom can induce significant changes in their properties [5]. Moreover, stable and high purity products free from $AuCl_4^-$ ion inclusions are required for the application of gold USNps and NCs in in vivo bio imaging tests. On the other hand, purification by dialysis and rinsing/centrifugation procedures frequently leads to destruction of surroundings, which stabilize NCs.

To produce Au NCs, the method which involves ablating the material with plasma under high pressure has been reported by Smalley et al. three decades ago [6]. Later, this method has been successfully applied to synthesize close-shell Au_{13}, Au_{55} (n=3) and Au_{147} (n=4) USNps [7]. Schmidt et al. [8] have prepared Au USNps with quite uniform size of 1.4 nm by the reduction of Ph_3PAuCl with highly toxic diborane in benzene. Similarly, 1.5 nm sized gold particles have been obtained by reduction of $AuCl_4^-$ with $NaBH_4$ in aqueous solution containing triphenylphosphine [9]. Numerous syntheses have been also reported for thiol-stabilized gold USNps, namely Au_{25} [10], Au_{38} [11,12], Au_{40} [13], Au_{68} [14], Au_{102} [15,16], Au_{144} [17], Au_{333} [18], and others [19]. To obtain nearly monodisperse Au USNps of 1.3 and 1.6 nm size, Kim et al. suggested the encapsulation in dendrimers by capping the cysteine as a bound ligand around USNps and examined the process in terms of size, composition and environment [20]. The synthesis of biocompatible, red-luminescent gold NCs with emission peak at 640 nm and QY≈6% has been first reported by Ying et al. [21]. The authors used encapsulation of Au(III) ions by thiol groups, present in cysteine residues, in alkaline solution of bovine serum albumin (BSA) and the subsequent reduction. Similarly, for cells bio imagining, Liu et al. [22] successfully prepared water-soluble fluorescent Au NCs capped with dihidrolipoic acid and modified with polyethylene glycol, BSA and streptavidin, demonstrating that these proteins are advantageous as reducing and stabilizing agents. During past several years, Au NCs have been also successfully synthesized using other proteins such as lysozyme [23,24], trypsin [25], pepsin [26], bovine [27] and human insulin [28] and horseradish peroxidase [29]. The formation of fluorescent Au NCs in protein-containing solutions was attributed to complexation of $AuCl_4^-$ ions to Au(I) and the subsequent reduction to Au^0 by tyrosine or tryptophan residues [30] and stabilization with cysteine residues, although exact formation and stabilization mechanisms are still an open question. Recently, the effects of size and amino acid contents in the several suitable proteins, namely bovine serum albumin, lysozyme, trypsin and pepsin, on the fluorescent properties of fabricated Au NCs have been investigated in detail demonstrating that photoluminescence spectrum, emission lifetime and photo stability depended on the concentration ratio of amine and tyrosine/tryptophan-containing residues [31]. It was also presumed that application of multiple proteins containing amine and thiol groups is a prerequisite to obtain stable, well fluorescent product [31]. However, it seems likely that fluorescent properties (intensity and wavelength of emitted light) of Au NCs, fabricated by protein-templating approach, depend also on the source, size and purity of protein, pH of solution applied and concentration

ratio of all reaction counterparts. In addition, due to large molecular weight of proteins, the overall size of fluorescent Au NCs formed and stabilized in protein solutions can attain several tens of nanometres, which makes it difficult to preserve the composition and properties of the shells in in vivo environments. To avoid this problem, Bao et al. [32] reported the formation of blue-fluorescent Au NCs by templating $AuCl_4^-$ ions in the biological small-sized buffer MES and L-ascorbic acid solution. However, in this case the yield of Au NCs was poor due to the concomitant formation of Au Nps.

Herein, we report for the first time the cost-effective synthesis of Au NCs by reduction of chloroauric acid with amino acid food supplement (AAFS) resulting in the formation of stable and biocompatible NCs, with characteristic intense red photoluminescence (PL), peaked at 660 to 705 nm, and average lifetime of up to several μs. We note that application of cheap amino acid cocktails, instead of earlier proposed pure and significantly expensive BSA [21], insulin [27,28] and others, makes this synthesis very attractive. We also found that synthesized Au NCs after dialysis are non-toxic and covered with protein-based shells quite similar with Au@BSA NCs. To assess viability and versatility of synthesized products, in vitro experiments were performed by incubation with two breast cancer cell lines differing in malignancy.

2. EXPERIMENTAL SECTION

2.1. Materials. All tested amino acids (purity ≥ 99.0%) in powder form, glucose and $HAuCl_4$ were purchased from Sigma-Aldrich Co. High quality amino acids food supplement INTRA BCAA'S was purchased from Stockton-on-Tees. Analytical grade NaOH was purchased from Reachem (Slovakia). Ultra-pure water (18 MΩ cm) was obtained using Water purification system and used in all experiments. The pH of the resulting solutions was adjusted by addition of 1.0 M NaOH solution under continuous stirring.

2.2. Synthesis of amino acid-encapsulated gold nanoclusters. In this study, the red-fluorescent gold nanoclusters (AuNCs) were synthesized through the amino acids food supplement (AAFS) templating and reduction of $AuCl_4^-$ in alkaline medium at a physiological temperature of 37 °C. In a typical synthesis, 7 mL of an aqueous solution were prepared by dissolving 0.140 g of AAFS together with $HAuCl_4$ and NaOH to make pH within 10.0 to 13.5. Resulting concentrations of amino acids and $HAuCl_4$ were 5 mg/mL and 3 μM/mL, respectively. After the addition of base, the synthesis reaction was conducted at 37 °C for up to 20 h. Similarly, various mixed compositions of pure amino acids with the total amount of 5 mg/mL with and without various additives, such as glucose, starch and citric acid, were tested. For comparison, bovine serum albumin-encapsulated gold clusters were also synthesized under the same conditions. The resultant clear yellow-coloured Au NCs solutions were examined using high resolution transmission electron microscopy, AFM, UV-vis and fluorescence spectroscopy.

2.3. Spectroscopic characterization of Au NCs. Absorption spectra of investigated Au NCs solutions were measured using the Jasco V670 spectrophotometer. Hellma Optik (Jena, Germany) quartz cuvette with 1 cm length optical path was used for all optical measurements. Photoluminescence spectra and photoluminescence decay kinetics were measured with a time-correlated single photon counting spectrometer Edinburgh-F900 (Edinburg instruments, United Kingdom). A picosecond pulsed diode lasers EPL-375, EPL-405, EPL-470 emitting picosecond duration pulses were used for the excitation. "FAST" software package for the advanced analysis of Au NC FL multi-exponential decay kinetics was used. The stationary photoluminescence properties of the synthesized Au NCs solutions were registered on Cary Eclipse spectrophotometer (Varian Inc., USA). All photoluminescence spectra were corrected for the instrument sensitivity.

The quantum yield (QY) of gold nanoclusters formation was calculated by comparing the fluorescence intensities of the sample to that of a standard laser dye 2-[2-[2-(4-Dimethylamino-phenyl)-vinyl]-6-isopropyl-pyran-4-ylidene]-malononitrile (DCM) in methanol, which QY was 33-34%.

2.4. Live cell imaging and confocal laser scanning microscopy. Human breast cancer cell lines MCF-7 (ECCC No. 86012803) and MDA-MB-231 (ATCC No. HTB-26TM) were purchased from European Collection of Cell Cultures and American Type Culture Collection, respectively. The cells were cultured in Dulbecco's Modified Eagle Medium (DMEM), which was supplemented with 10% fatal bovine serum, 100 U/ml penicillin and 100 mg/ml streptomycin. All media and supplements were purchased from Gibco (UK). Cells were cultured in 25 cm^2 culture dishes in a humidified 37 °C, 5% CO^2 atmosphere and sub cultured twice a week. To evaluate Au NCs accumulation, MCF-7 and MDA-MB-231 cells were plated in 8-well chambered cover-slips (Nunc, USA) at an appropriate density (5 x 104 cells per well) and cultured in a CO_2 incubator for 24 hours. Next day cells were washed three times with phosphate-buffered saline (pH 7.4) (PBS) and treated with 3 mM/L Au NCs for 24 hours. After treatment, MCF-7 and MDA-MB- cells were routinely rinsed 3 times with DME medium and then were analysed by the confocal Nikon Eclipse TE2000 C1 Plus laser scanning microscope equipped with CO2 Microscope Stage Incubation System (OkoLab, Italy). Measurements were done using 60×/1.4 NA oil immersion objective (Plan Apo VC, Nikon, Japan) and 488 nm argon-ion laser. To visualize Au NCs photoluminescence, the 621-755 nm band pass filter was applied. The images were further processed using the EZ-C1 Bronze version 3.80 (Nikon, Japan) and ImageJ 1.41 software (NIH, USA). An Atomic force microscope (Dimension 3100a Nanoscope, Veeco Instruments Inc.) was used to image the fabricated films.

3. RESULTS SECTION

In the first setup, several currently popular amino acid food supplements, namely Anabolic Whey protein (AWP), Natural Whey protein (NWP), 100% Milk Complex (MC), 100% Whey protein professional (WPP), and Branched Amino Acids

supplement (BCAA'S), can be purchased in the market, were tested as reducers of chloroauric acid in an alkaline medium and physiological temperature (37 ºC). It is of note that after 20 h synthesis, the red-fluorescent Au NCs were obtained only in the case of BCAA'S. In all other cases, to obtain even light reddish excitation, the synthesis ought to be continued by week (Fig. 1). Therefore, further investigations were carried out with BCAA'S food supplement.

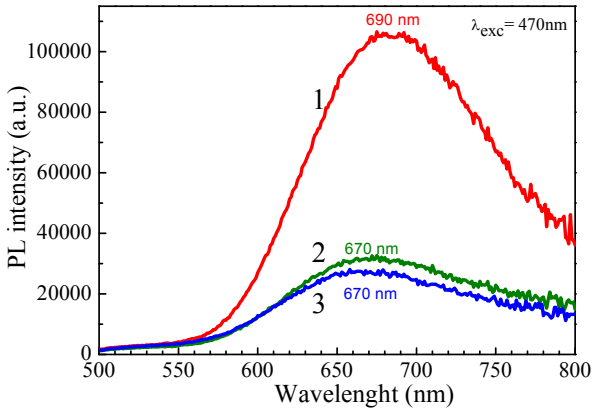

Figure 1. Fluorescence spectra of Au NCs formed from the alkaline (pH=12.0) solutions containing 3 μM/mL $HAuCl_4$ and 20 mg/mL amino acid food supplements: (1) BCAA'S, (2) 100% Milk complex and (3) 100% Whey protein professional after 20 (1) and 200 h (2,3) synthesis at 37 ºC.

In order to find the optimal conditions for the synthesis of Au NCs in the solution of BCAA'S food supplement and $HAuCl_4$ at physiological temperature of 37 ºC, the dependence of PL properties such as intensity and wavelength range of the obtained products on the variation of the content of all precursors and pH was investigated. Figs. 2a and 2b depict the absorption and PL spectra of light yellow coloured solutions obtained after reduction of 3.0 mM/L $HAuCl_4$ with different contents of BCAA'S and pH value, respectively, after 20 h synthesis. Judging from the intensity of red PL it seems that AuNCs with the maximum fluorescence emission in the range between 670 and 690 nm are synthesized in the solution containing 16-20 mg/mL of BCAA'S (Fig. 2a, curves 3 and 4) at pH≈12.0 (Figure 2b, curve 3). If concentration of BCAA'S exceeds 20 mg/mL, the PL intensity of Au NCs decreases and the peak shifts by 10 nm towards higher wavelengths region (Fig. 2a, curve 5). When concentration of BCAA'S was lower than 8 mg/mL, formation of stable Au NCs band was not observed et all. Besides, in contrast to the synthesis of Au NCs from the other reported protein solutions [22-31], only weak red PL in the 660 to 770 nm spectral region was determined for the BCAA'S synthesis products formed in the solutions with pH 10.0 and 11.0 (Fig. 2b, PL spectrum 1). Note that increase of pH to 12.0, resulted in an obvious increase of UV light absorption in the longer wavelengths region (Fig. 2b). However, further increase of pH, resulted in the significant absorption decrease perhaps due to conformational changes of BCAA'S proteins resulting in the spatial redistribution of fluorophores.

Fig. 3a shows photoluminescence excitation spectrum and PL spectra of BCAA'S-mediated Au NCs formed in the optimized solution under various excitation wavelengths. As seen, the PL intensity of the obtained Au@BCAA'S NCs and emission light peak strongly depend on the excitation light decreasing with λ_{exc}. Again, the photoluminescence excitation spectrum of Au NCs solution (λ_{em}=690 nm) has a band at 510 nm and a gradual slope towards the longer wavelength region. In addition, photoluminescence excitation spectrum does not coincide with absorption spectrum of Au@BCAA'S NCs.

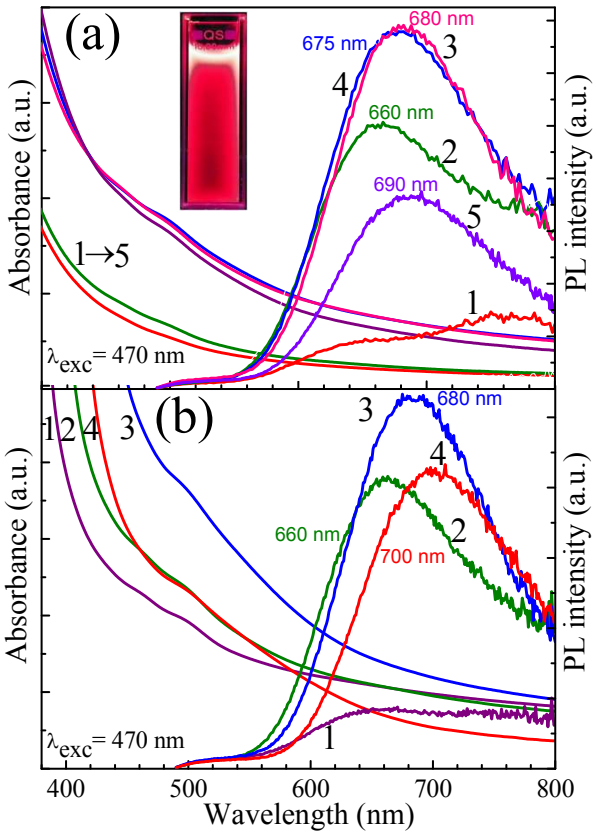

Figure 2. (a) Absorption and PL spectra of Au NCs formed via BCAA'S food supplement-mediated synthesis in the 3.0 μM/mL $HAuCl_4$ solution containing: 8 (1); 12 (2); 16 (3); 20 (4) and 24 (5) mg/mL BCAA'S; all kept at a pH = 12.2 and 37 °C for 20 h. (b) Absorption and PL spectra of Au clusters fabricated in 3.0 μM/mL $HAuCl_4$ solution containing 20 mg/mL BCAA'S at pH: 11.0 (1); 11.5 (2) 12.0 (3) and 12.5 (4) at 37 ºC for 20 h. λ_{exc}= 470 nm. In the Inset, the colour of fabricated Au NCs under UV irradiation is shown.

The lifetime of red PL of Au@BCAA'S NCs with non-exponential decay typically exceeds several μs (Fig. 3b). Such long lifetimes are not typical for Au NCs fabricated via templating of $AuCl_4^-$ in the similar alkaline solutions using proteins such as BSA [22,24] and others [31] but are close to lifetimes of lipoic acid-protected Au NCs, synthesized recently [33].

It was found that the PL spectrum of BCAA'S-mediated Au NCs solution shifted slightly from the peak position of 705 nm to 680 nm upon dilution and after six fold dilution integral intensity decreased about 14 times (Fig. 4a). It is worth noticing that neutralizing of as-formed Au@BCAA'S NCs solutions by addition of citric acid, blue-shifted the PL peak position only insignificantly, namely about 4.0 nm/pH. At the same time, the PL intensity and lifetime of Au NCs changed only slightly (Fig. 4b and 4c), allowing to expect such photoluminescence lifetimes also after insertion of Au NCs into bio entities for cells imaging.

The quantum yield (QY) of ~7.0% was obtained for red-luminescent Au@BCAA'S NCs fabricated under the optimized conditions. Note that such QY is higher than reported for red-luminescent Au NCs synthesized by BSA protein-directed reduction of chloroauric acid [21]. Furthermore, the obtained in this study Au@BCAA'S NCs typically have photoemission peak position at from 670 to 705 nm, indicating on the inclusion of

Au27-Au29 atoms in each nanocluster, based on the spherical Jellium model [34].

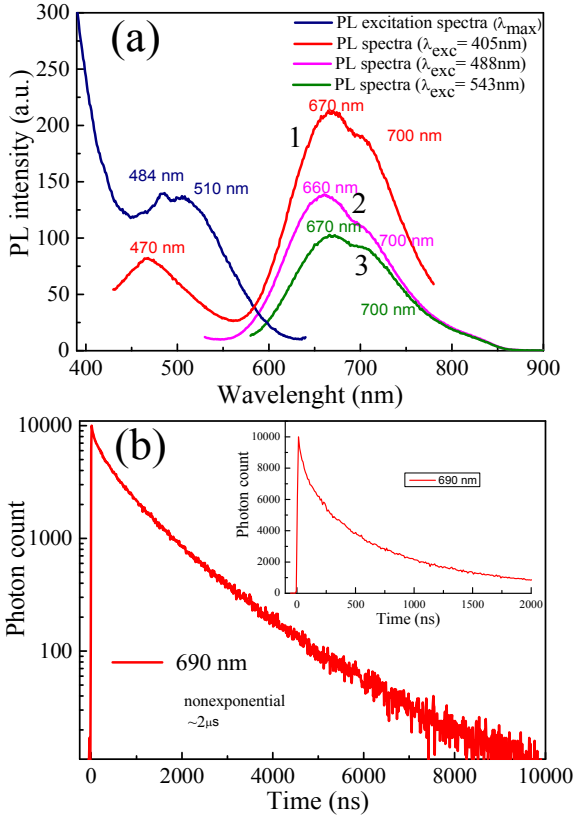

Figure 3. (a) Variation of the PL spectra of BCAA'S-mediated Au NCs formed in the optimized solution with the excitation light wavelength (nm): 405 (1); 488 (2) and 543 (3). (b): Typical photoluminescence intensity decay for BCAA'S-mediated Au NCs at PL band peak position 690 nm.

Fig. 5 depicts variation of absorbance and PL spectra of Au@BCAA'S NCs solution upon dialysis for 24 and 48 hours. As seen, the dialysis results in the significant increase of PL intensity, light absorption decrease and blue-shift of PL spectra peak from 700 nm to 680 nm. The analysis of solutions before and after dialysis have showed that only 42.5% of chloroauric acid was consumed for Au@BCAA'S NCs formation under the optimized synthesis conditions determining a lower PL intensity of these NCs with respect to Au@BSA NCs. However, we found in this study that addition of some amino acids to the synthesis solution of BCAA'S and chloroauric acid can significantly increase or decrease the PL intensity of the synthesized NCs (Fig. 6) and the yield of red-luminescent gold clusters. The most effective influence was obtained using leucine, serine and glutamic acid whereas the addition of cysteine hindered the formation of red luminescent gold NCs. On the other hand, the addition of cysteine resulted in the formation of blue fluorescent gold clusters possessing emission peak at 495 nm (spectrum 5 in Fig. 6).

The AFM topography images of dialyzed Au@BCAA'S NCs and Au@BSA NCs synthesized according to [21], for comparison, are shown in Fig. 7. From these observations, the average size of gold clusters stabilized with BCAA'S is quite similar to ones formed via BSA reduction of chloroauric acid under a same conditions, while the calculated size distribution histograms demonstrated some larger Au@BCAA'S NCs with a main size of 2.7 nm instead of ~2.0 nm [21].

The FTIR spectra of the BCAA'S, BSA and corresponding gold nanoclusters Au@BCAA'S and Au@BSA before and after dialysis were also studied to compare the composition of shells stabilized these NCs. As seen (Fig. 8), the FTIR spectra of Au@BCAA'S and Au@BSA NCs after the complete purification by dialysis for 48 h are quite similar implying on the compositional similarity of shells stabilizing these NCs. The bands corresponding to amide I (CO stretch) in a vicinity of 1658-1643 cm^{-1} and amide II (CN stretch and NH in-plane) band in a vicinity of 1515-1544 cm^{-1} [33] are clearly seen in the spectra of both clustered products.

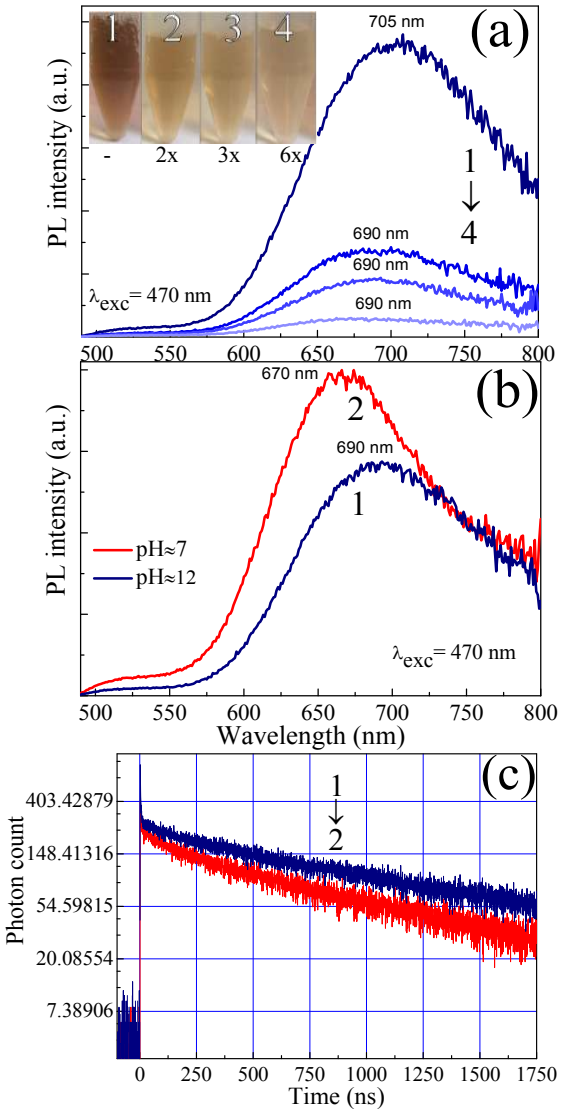

Figure 4. Variation of the PL spectra of 3.0 μM/mL Au NCs solution mediated with 20 mg/mL BCAA'S upon dilution (a) and neutralization (b). The Inset in (a) shows the colour of Au NCs solutions before and after dilution by the extent indicated under solar light illumination. In (c): the emission light intensity decay of corresponding Au NCs (b) solutions under excitation with λ_{exc} of their peak positions.

Besides, in the both cases, the dialysis of NCs results in the more prominent and stronger vibrations of these bands. The exact reasons of this phenomenon is not clear and probably can be linked with more ordering distribution of the corresponding protein residues around gold nanocrystal after dialysis. To the end, the wide vibration band appearing at ~700 cm^{-1} in all samples was assigned to $-NH_2$ and –NH wagging and that of 1398 ± 1 cm^{-1} to C=O stretching of COO-.

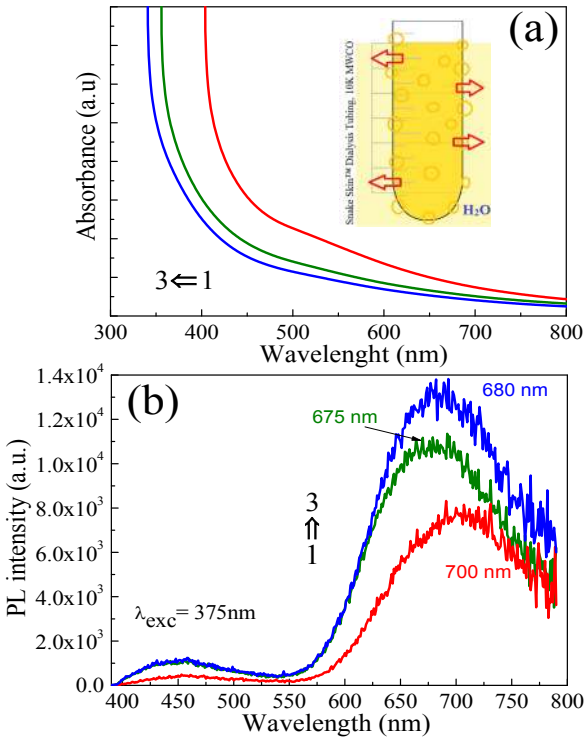

Figure 5. Typical absorption (a) and PL (b) spectra of Au@ BCAA'S clusters before (1) and following the dialysis for 24 h (2) and 48 h (3). λ_{exc}= 470 nm. In the Inset, the scheme of dialysis is shown.

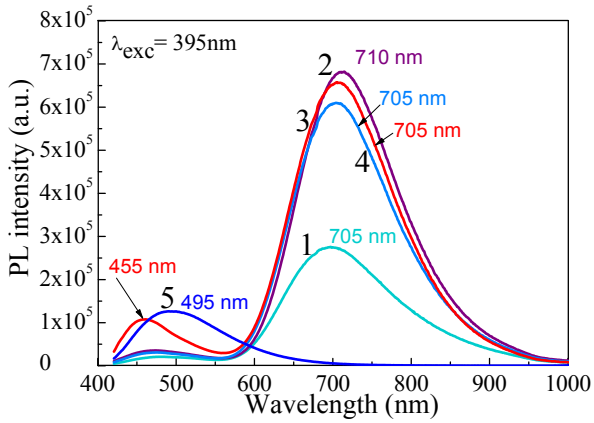

Figure 6. PL spectra of gold clusters fabricated at 37 °C for 20 h in the solution containing 15 mg mL^{-1} BCAA'S and 3.0 μM/mL $HAuCl_4$ without (1) and with addition of 15 mM Leu (2), Ser (3), Glutamic acid (4) and Cis (5).

The data presented in Table 1 revealed a significantly lower concentration of most amino acids (AA), except Ala, Glu and Val, in the BCAA'S additive with respect to ones in other tested herein food supplements can be used for red-photoluminescent Au NCs formation from alkaline medium at physiological temperature of 37 ºC. However, the percentage of branched AA (Leu, Ileu and Val) in the BCAA'S approximated to 30% from the total contamination of all AA, what is about 50% more than in the 100% MC and 100% MPP food supplements.

Again, based on the recent discussion [31], the lower concentration of –S- and –SH containing entities in BCAA'S, as well as Thr and Trp, not allow us to explain the significantly higher efficiency of BCAA'S, with respect to 100% MC and 100% MPP usage.

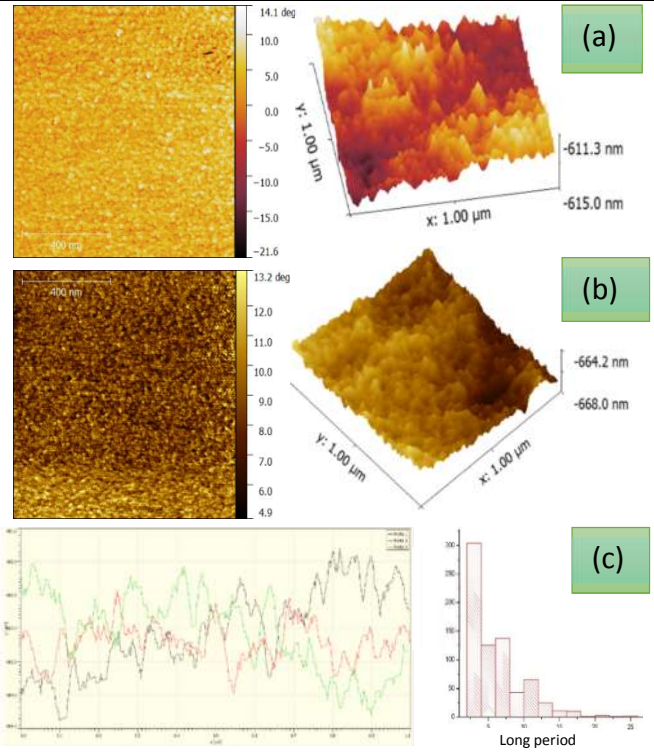

Figure 7. The AFM and 3D deflection images of gold clusters fabricated using food supplement BCAA'S (a) and BSA reducers (b) under a same synthesis and dialysis conditions. In (c) the size distribution histogram calculated from the corresponding profile-grams for Au@BCAA'S NCs (left side) is presented.

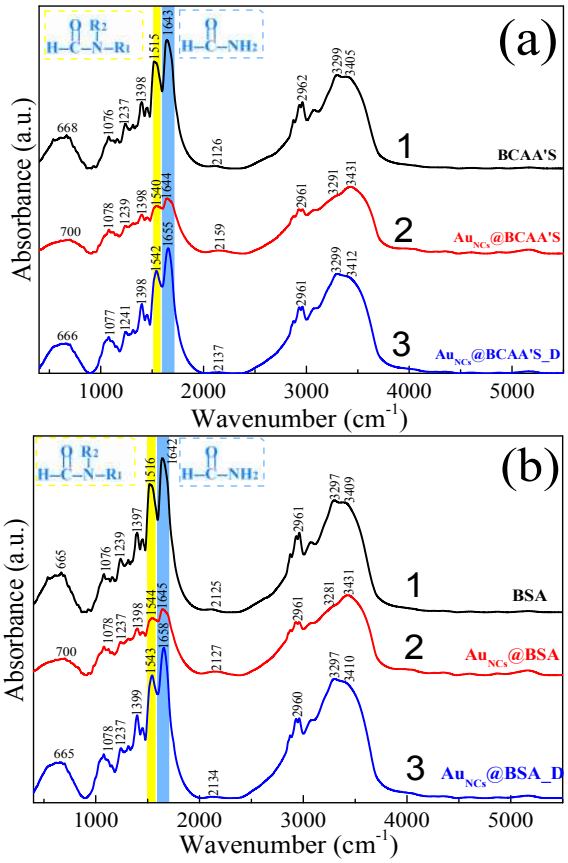

Figure 8. (a) FTIR spectra of pure BCAA'S (1), and BCAA'S-encapsulated Au NCs before (2) and after (3) dialysis. (b) a same for pure BSA protein (1) and Au NCs generated by BSA-encapsulated Au NCs before (2) and after (3) dialysis.

Thence, it can be inferred that other BCAA'S components, such as carbohydrates, could be responsible for the higher reduction

capability of BCAA'S. At a same time, it can be deduced that except –S- and –SH containing AA, others can also stabilize Au NCs bonding via amino groups to gold, as predicted in [31].

To assess which amino acid favoured the formation of red-fluorescent Au NCs, twenty individual amino acids in 0.15 mol/L concentration were incubated each with 3.0 μM/mL $AuCl_4^-$ alkaline solution at pH = 12 and 37^{0}C for 20 hours. The results obtained in these experiments indicated that only in the solution containing histidine amino acid, bluish-green fluorescent Au NCs without larger Au nanoparticles were formed (Fig. 9a, plots 1and 1'). However, the photoluminescence intensity of the obtained Au@histidine NCs solution was exceptionally poor and decayed rapidly (Fig. 9b). Note that similar results were obtained recently by creating fluorescent Au@His NCs capped with molecules of organic fluorescent dye MPA in the acidic solution, emphasizing the crucial role of histidine imidazole group [35].

No red-fluorescent Au NCs were formed by the templating of $AuCl_4^-$ in the alkaline solutions containing single amino acid. On the other hand, the reduction of $AuCl_4^-$ ions to the metallic state was observed in the solutions containing methionine, isoleucine, leucine, alanine, threonine, asparagine, lysine, aspartate and phenylalanine, forming plasmonic Au nanoparticles (Fig. 10 a). The excitation of resulting solutions with UV light resulted mainly in the blue or bluish-green luminescence (Fig. 10b). As from early report [24], this effect could be explained by the formation of exceptionally small Au clusters composed of only several gold atoms.

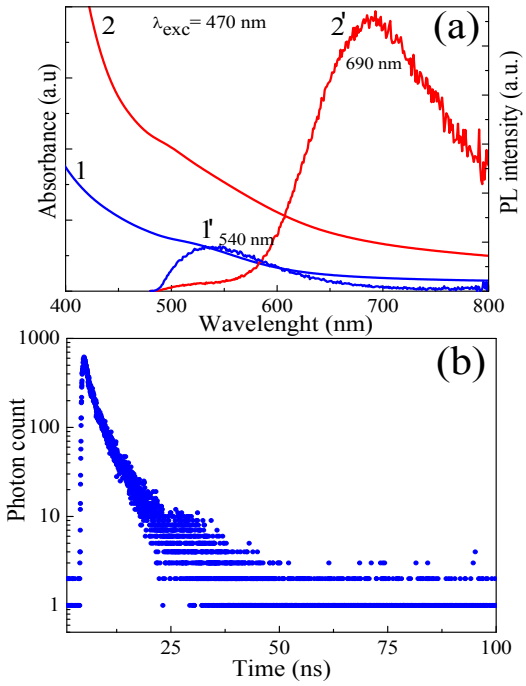

Figure 9. (a) Typical absorption (1, 2) and photoluminescence (1', 2') spectra of gold clusters produced by reduction of 3.0 μmol/mL $HAuCl_4$ in the alkaline medium (pH = 12.0) with 20 mg/mL histidine (1) and 20 mg/mL BCAA'S (2) at 37 ^{0}C for 20 h. (b) Photoluminescence decay plot for Au@histidine NCs under excitation with λ_{exc} = 375 nm light.

Table 1. The contents of indicated amino acids in a 100 g of tested food supplements.

Food supplement	Amino acid																		
	Ala	Arg	Asp	Cys	Glu	Gln	Gly	His	Ileu	Leu	Lys	Met	Phe	Pro	Ser	Thr	Trp	Tyr	Val
100% MC	3.34	1.47	7.63	1.54	-	12.67	0.98	1.19	4.48	7.42	6.72	1.54	2.17	3.92	3.22	4.62	0.98	1.86	4.13
100% WPP	3.37	1.78	7.6	2.06	-	14.7	1.28	1.24	4.7	8.28	7.46	1.6	2.23	4.23	3.73	4.8	1.27	2.36	4.34
BCAA'S	3.99	0.39	2.1	0.49	3.4	-	0.3	0.7	1.34	3.96	2.97	0.38	0.58	1.21	0.96	1.36	0.42	0.52	3.08

In the subsequent experiments, solutions of several mixed amino acids were prepared with 3.0 μM/mL $HAuCl_4$ and NaOH up to pH = 12.0 and left at 37 ºC for 5, 10, 15, 20, 25 and 30 h. The cocktails of amino acids (AA) with the total content of 30.0 mg/mL were composed from the following groups: (A) branched AA (leucine, isoleucine, valine); (B): -S- and –SH groups containing AA (methionine, cysteine), (C): =NH and =N- groups containing AA (histidine, arginine, tryptophan, proline) and (D): two COO- groups containing AA (aspartic, glutamic) at various concentration ratios. In this way, it was found that formation of fluorescent Au NCs in the solutions containing dominant amount of branched AA, e.g. 30%, like in the tested BSAA'S case, proceeds very slowly. The resultant products, even after 30 h long synthesis, demonstrated quite weak photoluminescence in comparison with Au NCs formed in the BCAA'S-containing solution at the same pH and other conditions. Variations in the composition of AA cocktail by increasing the content of sulphur- as well as nitrogen-containing AAs up to 30% resulted mainly in the formation of non-red-fluorescent solutions, implying that other reductants could be responsible for the formation of red-fluorescent Au NCs in the AAFS-templated solutions. With this in mind, the influence of typical carbohydrates such as glucose and sucrose, which are the constituents of food supplement, was also tested herein. From these experiments, it was found that addition of up to 10% of carbohydrates to the synthesis solution composed of histidine and $HAuCl_4$ as well as AA mixture cocktails and $HAuCl_4$ results in the formation of 5 to 6 times more intense bluish-green fluorescence. Further increase in the concentration of glucose and sucrose up to 25% from the total content of AA, with other conditions being the same, led to the formation of more intense blue-fluorescent Au NCs under UV illumination. In these experiments, however, no red-photoluminescent Au NCs were formed. These experimental findings revealed the crucial role of amino acids and carbohydrates in the formation and encapsulation of red-photoluminescent Au NCs. Further investigations are in progress.

Cellular internalization behaviours of our red-luminescent BCAA'S-Au NCs were further visualized by fluorescence confocal microscope imaging in two human breast cancer cell lines with different degree of malignancy. After 24 h, MCF-7 and MDA-MB-231 cells internalized different amounts of Au NCs (Fig. 11).

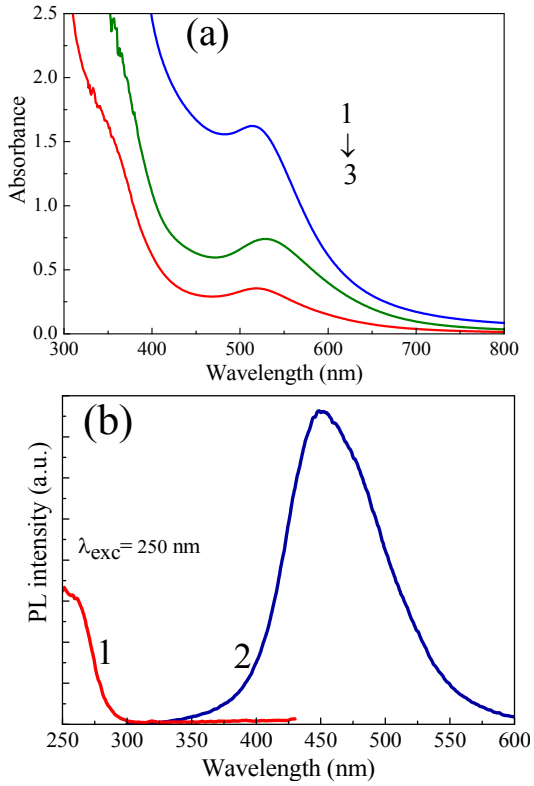

Figure 10. (a): UV-vis absorption spectra of 3.0 μmol/mL $HAuCl_4$ alkaline solutions (pH = 12.0) after 20 h of incubation with 0.15 mM/L alanine (1), threonine (2) and phenylalanine (3) at 37 °C. In (b) excitation (1) and photoluminescence (2) spectra of methionine templated 3.0 μmol/mL $AuCl_4^-$ solution kept at 37 ^{0}C for 20 h. In the Inset (b) the PL colour of as-formed Au NCs under UV illumination is shown.

No detectable intracellular uptake of Au NCs was observed in MCF-7 cells, however numerous bright red luminescent spots illuminating the cell cytoplasm were clearly observed in MDA-MB-231 cells after 1 h of incubation (data not shown) and their amount increased with incubation time (Fig. 11b). The granulated pattern of red photoluminescence of

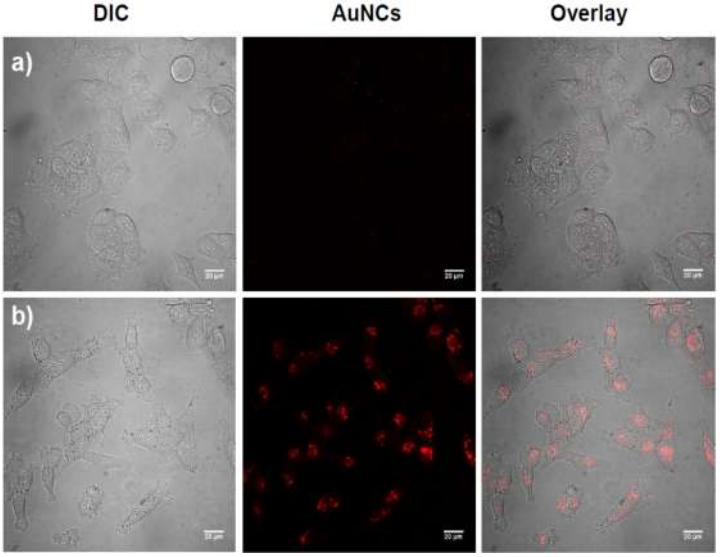

Figure 11. Confocal fluorescence microscopy images of MCF-7 (a) and MDA-MB-231 (b) cells incubated with Au NCs for 24 h. Images were captured in DIC mode and Au NCs channel. Scale bar: 20 μm.

Au NCs present inside MDA-MB-231 cells indicates that Au NCs were trapped in vesicular structures. Our previous studies with negatively charged nanoparticles demonstrated similar intracellular distribution pattern, which means that Au NCs were entrapped in intracellular vesicles and internalized into cells by endocytosis [36,37]. Note, that our recent results well satisfied with ones obtained investigating the accumulation of red-luminescent Au @BSA NCs in tumours MDA-MB-45 and Hela into the nude mice [38] showing the higher fluorescence intensity in the tumour areas after several hours post injection due to enhanced permeability and retention effect [39].

4. CONCLUSIONS

In this study, the formation of red-photoluminescent gold nanoclusters (Au NCs) were studied by the templating of $AuCl_4^-$ alkaline solutions with several food supplements composed of amino acids cocktails. We found that in the case of branched amino acids food supplement, BCAA'S, application the obtained Au NCs are characterized by good stability, intense red photoluminescence, peaked in the vicinity of 690 nm with surprisingly long lifetime attaining several microseconds and high quantum yield. In vitro investigations also implied that fabricated Au NCs tend to accumulate in more tumorigenic breast cancer cells (line MDA-MB-213) and are promising candidates for bio imagining.

The formation of red-photoluminescent Au NCs in the alkaline solutions of $AuCl_4^-$ containing individual amino acid as well as various amino acid cocktails with and without carbohydrates such as sucrose and glucose was also tested herein. In all cases, however, only blue- or bluish-green-emitting Au NCs, if at all, were formed.

We suspect that this study opens new direction for research in the green synthesis of biocompatible Au NCs using cost-effective amino acid food supplements instead of pure proteins and can be useful for future fluorescent nanoclusters technologies.

5. REFERENCES

[1]. Kim B.H., Hackett M.J., Park, J., Hyeon T. Synthesis, Characterization, and Application of Ultra small Nanoparticles, *Chemistry of Materials*, 26, 59-71, **2014**.

[2]. Li Y., Liu S., Yao T., Sun Z., Jiang Z., Huang Y., Cheng H., Huang Y., Jiang Y., Xie Z., Pan G., Yan W., Wei S. Controllable synthesis of gold nanoparticles with ultra-small size and high monodispersed via continuous supplement of precursor, *Dalton Transactions*, 41, 11725-11730, **2012.**

[3]. Zheng Y., Gao S., Jing J. Y. Synthesis and Cell-Imaging Applications of Glutathione-Capped CdTe Quantum Dots, *Advanced Materials*, 19, 376-380, **2007**.

[4]. Hardman R.A Toxicological Review of Quantum Dots: Toxicity Depends on Physicochemical and Environmental Factors, *Environmental Health Perspectives*, 114, 165-172, **2006**.

[5] Gilb S., Weis P., Furche F., Ahlrichs R., Kappes M.M. Structures of small gold cluster cations Ion mobility measurements versus density functional calculations, *The Journal of Chemical Physics*, 116, 4094-4101, **2002.**

[6] Kroto H.W., Heath J.R., O'Brien G.C., Curl R.F., Smalley R.E., C60: Buckminsterfullerene, *Nature*, 318, 162-163, **1985**.

[7] Schmid G. Metal clusters and cluster metals, *Polyhedron*, 7, 2321-2329, **1988.**

[8] Schmid G., Pfeir R., Boese R., Bandermann F., Meyer S., Calis G.H. M., van der Velder, J. W. A. $Au_{55}[P(C_6H_5)_3]_{12}CI_6$ — ein Gold cluster un gewöhnlicher Größe, *Chemische Berichte*, 114, 3634-3642, **1981**.
[9] Weare W.W., Reed S.M., Warner M.G., Hutchison J.E. Improved Synthesis of Small (dCORE ≈ 1.5 nm) Phosphine-Stabilized Gold Nanoparticles, *Journal of the American Chemical Society,* 122, 12890-12891, **2000**.
[10] Schaaff T.G., Whetten R.L. Giant, Gold−Glutathione Cluster Compounds: Intense Optical Activity in Metal-Based Transitions, *The Journal of Physical Chemistry B,* 104, 2630-2641, **2000**.
[11] Pei Y., Gao Y., Zeng X.C. Structural Prediction of Thiolate-Protected Au38: A Face-Fused Bi-icosahedral Au Core, *Journal of the American Chemical Society*, 130, 7830-7832, **2008**.
[12] Toikkanen O., Ruiz V., Ronnholm G., Kalkkinen N., Liljeroth P., Quinn B.M., Synthesis and Stability of Monolayer-Protected Au_{38} Clusters, *Journal of the American Chemical Society,* 130, 11049-11055, **2008.**
[13] Qian H., Zhu Y., Jin R., Isolation of Ubiquitous $Au_{40}(SR)_{24}$ Clusters from the 8 kDa Gold Clusters, *Journal of the American Chemical Society*, 132, 4583-4585, **201.**
[14] Dass A. Mass Spectrometric Identification of $Au_{68}(SR)_{34}$ Molecular Gold Nanoclusters with 34-Electron Shell Closing, *Journal of the American Chemical Society,* 131, 11666-11667, **2009.**
[15] Jadzinsky P.D., Calero G., Ackerson C.J., Bushnell D.A., Kornberg R.D., Structure of a Thiol Monolayer-Protected Gold Nanoparticle at 1.1 Å Resolution, *Science*, 318, 430-433, **2007**.
[16] Levi-Kalisman Y., Jadzinsky P.D., Kalisman N., Tsunoyama H., Tsukuda T., Bushnell, D.A., Kornberg R.D., Synthesis and Characterization of $Au_{102}(p\text{-}MBA)_{44}$ Nanoparticles, *Journal of the American Chemical Society,* 133, 2976-2982, **2011**.
[17] Qian H., Jin R., Controlling Nanoparticles with Atomic Precision: The Case of $Au_{144}(SCH_2CH_2Ph)_{60}$, *Nano Letters*, 9, 4083-4087, **2009.**
[18] Qian H., Zhu Y., Jin R., Atomically precise gold nanocrystal molecules with surface plasmon resonance, *Proceedings of the National Academy of Sciences,* 109, 696-700, **2012.**
[19] Shichibu Y., Negishi Y., Tsunoyama H., Kanehara M., Teranishi T., Tsukada T., Extremely High Stability of Glutathione-Protected Au_{25} Clusters Against Core Etching, *Small*, 3, 835-839, **2007.**
[20] Kim Y.-G., Oh S.-K., Crooks R.M., Preparation and Characterization of 1−2 nm Dendrimer-Encapsulated Gold Nanoparticles Having Very Narrow Size Distributions, *Chemistry of Materials,* 16, 167-172, **2004**.
[21] Xie J., Zheng Y., Ying J.Y., Protein-Directed Synthesis of Highly Fluorescent Gold Nanoclusters, *Journal of the American Chemical Society,* 131, 888-889, **2009.**
[22] Lin,C.-A. J., Yang T.-Y., Lee C.-H., Huang S.H., et al., Synthesis, Characterization, and Bio conjugation of Fluorescent Gold Nanoclusters towards Biological Labelling Applications, *American Chemical Society NANO*, 3, 395-401, **2009.**
[23] Wei H., Wang Z., Yang L., Tian S., Hou C., Lu Y., Lysozyme-stabilized gold fluorescent cluster: Synthesis and application as Hg^{2+} sensor, *Analyst*, 135, 1406-1410, **2010**.
[24] Chen T.-H., Tseng W.-L. (Lysozyme Type VI)-Stabilized Au 8 Clusters: Synthesis Mechanism and Application for Sensing of Glutathione in a Single Drop of Blood, *Small*, 8, 1912-1919, **2012.**
[25] Kawasaki H., Yoshimura K., Hamaguchi H., Arakawa R., *Analytical Sciences*, 27, 591-596, **2011**.
[26] Kawasaki H., Hamaguchi K., Osaka I., Arakawa R., pH-Dependent Synthesis of Pepsin-Mediated Gold Nanoclusters with Blue Green and Red Fluorescent Emission, *Advanced Functional Materials*, 21, 3508-3515, **2011**.
[27] Liu C., Wa H., Hsiao Y., Lai C., Cheng J.-T., Chou P.-T., et al.; Insulin-Directed Synthesis of Fluorescent Gold Nanoclusters: Preservation of Insulin Bioactivity and Versatility in Cell Imaging. *Angewandte Chemie International Edition,* 50, 7056-7060, **2011**.
[28] Garcia A.R., Rahn I., Johnson S., Patel R., Guo J., Orbulescu J., Micic M., Whyte J.D., Blackwelder P., Leblanc R.M., Human Insulin fibril-assisted synthesis of fluorescent gold nanoclusters in alkaline media under physiological temperature, *Colloids and Surfaces B: Biointerfaces*, 105, 167-172, **2013.**
[29] Wen F., Dong Y., Feng L., Wang S., Wang S., Zhang S., Horseradish Peroxidase Functionalized Fluorescent Gold Nanoclusters for Hydrogen Peroxide Sensing, *Analytical Chemistry*, 83, 1193-1196, **2011**.
[30] Xu Y., Pal Choudhury S., Qin Y., Macher T., Bao Y., Make Conjugation Simple: A Facile Approach to Integrated Nanostructures *Langmuir*, 28, 8767-8772, **2012.**
[31] Xu Y., Sherwood J., Gin Y., Crowley D., Bonizzoni M., Bao Y., The role of protein characteristics in the formation and fluorescence of Au nanoclusters, *Nanoscale,* 6, 1515-1524, **2014.**
[32] Wintzinger L., An W., Turner C.H., Bao Y., Synthesis and Modelling of Fluorescent Gold Nanoclusters, *Joshua*, 7, 24-27, **2010**.
[33] Shang L., Stockmar F., Azadfar N., Nienhaus G.U., Intracellular Thermometry by Using Fluorescent Gold Nanoclusters, *Angewandte Chemie International Edition,* 52, 11154-11157, **2013.**
[34] Zheng J., Zhang C.W., Dickson R.M., Highly Fluorescent, Water-Soluble, Size-Tunable Gold Quantum Dots, *Physical Review Letters*, 93, 077402, **2004.**
[35] Chen H., Li B., Wang C., Zhang X., Cheng Z., Dai X., Zhu R., Gu Y. Characterization of a fluorescence probe based on gold nanoclusters for cell and animal imaging, *Nanotechnology,* 24, 055704, **2013**
[36] Karabanovas, V., Zitkus, Z., Kuciauskas, D., Rotomskis, R., Valius, M. Surface Properties of Quantum Dots Define Their Cellular Endocytic Routes, Mitogenic Stimulation and Suppression of Cell Migration, *Journal of Biomedical Nanotechnology*, 10, 775-786, **2014**.
[37] Damalakiene L., Karabanovas V., Bagdonas S., Valius M.,R. Rotomskis R. Intracellular distribution of nontargeted quantum dots after natural uptake and microinjection, *Journal of International Journal of Nanomedicine*, 8, 555-568, **2013.**
[38] Wu X., He X., Wang K., Xie C., Zhou B., Qing Z., Ultrasmall near-infrared gold nanoclusters for tumour fluorescence imaging in vivo, *Nanoscale*, 2244-2249, **2010.**
[39] Choi H.S., Liu W.H., Misra P., Tanaka E., Zimmer J.P., Ipe MG, Bawendi M.G., Frangioni J.V., *Biotechnology,* 25, 1165-1170, **2007**.